Supporting Information

Wang et al. 10.1073/pnas.1500408112

SI Materials and Methods

Animals. Female outbred Swiss Webster mice at 6~8 wk of age were purchased from Charles River Laboratories, and C57BL/6J and Capaspase-1$^{-/-}$ mice from Jackson Laboratories. IRF3$^{-/-}$, IRF7$^{-/-}$, STING$^{-/-}$, and MyD88/TRIF$^{-/-}$ mice were kind gifts of T. Taniguchi, Tokyo University, Tokyo (1, 2), G. Barber, University of Miami, Miami (3), and R. Medzhitov, Yale University, New Haven, CT, respectively. MHC II-EGFP mice expressing MHC class II molecule infused into enhanced green fluorescent protein (GFP) were a kind gift from M. Boes and H. Ploegh, Harvard Medical School (4). Male Yorkshire pigs at 4 mo of age were obtained from the Teaching and Research Resources at Tufts University. The animals were housed in the pathogen-free animal facilities of Massachusetts General Hospital (MGH) in compliance with institutional, hospital, and NIH guidelines. All studies were reviewed and approved by the MGH Institutional Animal Care and Use Committee.

Laser. An FDA-approved nonablative fractional laser, PaloVia, was used in mice (PaloVia Skin Renewing Laser, Palomar Medical Technologies). This device emits a 1,410-nm laser light and two passes at medium density were used to generate MTZs at the inoculation site (5). Pigs were treated with one pass of Fraxel SR-1500 laser (Solta Medical), with 17% coverage, 93 MTZs cm^{-2} per pass, and 35 mJ per microbeam (5).

Influenza Viruses and Vaccines. Pandemic A/California/7/2009 H1N1 influenza virus was obtained from American Type Culture Collection (ATCC, #FR-201). Influenza A Viruses were obtained through BEI Resources, National Institute of Allergy and Infectious Diseases, NIH, including A/Puerto Rico/8/1934 H1N1 (NR-348), A/New Caledonia/20/1999 H1N1 (NR-41799), and A/Aichi/2/68 H3N2 (NR-3177) viral strains. The viruses were expanded in 10-d-old embryonated chicken eggs at 35 °C for 3 d, harvested, and purified by sucrose gradient ultracentrifugation, and frozen at −80 °C until use. Viral quantities were determined with a 50% tissue culture infectious dose (TCID50) in Madin–Darby canine kidney cells (MDCK, ATCC, CCL-34). To challenge mice, the virus was adapted in mice for three cycles of intranasal instillation-lung homogenate preparation and infectivity of the resultant virus in mice was assayed by a LD50 following a standard protocol. Inactivated influenza vaccines were made by inactivating purified PR8 viruses with 0.024% formaldehyde at 4 °C for one week, followed by dialysis against PBS.

Fabrication of Microneedle Arrays. Microneedle arrays were prepared as described (6, 7). Compunds 1-vinyl-2-pyrrolidinone and 2, 2-Azobis (2-methyl-propionitrile) were obtained from Sigma-Aldrich, SU-8 2150, propylene glycol monomethyl ether acetate (PGMEA) and Trichloro (1H, 1H, 2H, 2H-perfluorooctyl) silane (Fluorosilane), from MicroChem, and polydimethylsiloxane (PDMS, Sylgard 184) from Dow Corning. A female microneedle mold was fabricated using a soft lithographic process with SU-8 2150 epoxy-based negative photoresist. Photomasks with different microneedle densities were placed on the surface of UV light-sensitive SU-8-coated silicon wafer, followed by rotational exposure to the UV light (UV light, 365 nm, 10 W/cm^2) for 200 seconds at an angle of 20°. The microneedle arrays were born under the mask pattern. After a propylene glycol monomethyl ether acetate (PGMEA) wash, SU-8 MNs molds were fabricated. The silicone elastomer base and curing agent of PDMS were mixed and then poured onto the SU-8 mold. Having de-gassed and cured at 65 °C, the PDMS MNs were peeled off, treated with fluorosilane via gas-phase deposition to increase surface hydrophobicity of the conical cavities. The PDMS microneedle array was used to generate another female PDMS array mold following a similar procedure. To prepare polyvinylpyrrolidone (PVP) MNs encapsulating indicated vaccines, a mixture of vinylpyrrolidone, free radical initiator azobisisobutyronitrile, and lyophilized influenza viruses or bacillus Calmette–Guérin vaccine was placed onto the surface of the second female PDMS microneedle mold. After vacuum for 5 min, a second solution containing vinylpyrrolidone and azobisisobutyronitrile was added on the same place to form the patch base following removal of the resident vaccine on the surface. Upon polymerization by irradiation with UV light (300 nm), the PVP MNs were obtained with a height of MNs at 600 μm, a base diameter of 200 μm each, and 6 × 9 MNs at varying densities.

Histological Examination. A MNs containing 10 μg of bacillus Calmette–Guérin vaccine was applied into the skin of C57BL/6 mice in the presence or absence of NAFL treatment. For ID injection control, one bacillus Calmette–Guérin-MNs was dissolved in 20 μL of PBS and then ID injected into mice. The tissue at the inoculation site was dissected at indicated times, fixed, and stained by a standard H&E procedure. The slides were scanned and analyzed by NanoZoomer (Hamamatsu).

Intravital Confocal Imaging. The lower dorsal skin of mice was treated with NAFL followed by insertion of MNs comprised of 5 μg OVA-AF647. OVA in the epidermis and dermis was imaged by intravital two-photon confocal microscopy (Olympus FV-1000) as described (8). Three-D reconstruction was used to quantify OVA fluorescence by Image J software. For dsDNA imaging, 100 μL of DRAQ7 (10 μM) was injected s.c. beneath the NAFL-treated site of MHC II-EGFP transgenic mice. dsDNA released from NAFL-injured cells and accumulation of APCs were then imaged by two-photon confocal microscopy.

Quantification of OVA$^+$ APCs in the Draining Lymph Nodes. Draining lymph nodes were collected and single-cell suspensions were prepared from MHC II-EGFP transgenic mice receiving OVA-AF647-MNs in the presence or absence of NAFL and analyzed by flow cytometry as described (9). The data were analyzed by FlowJo software.

Immunizations and Challenges. The lower dorsal skin of mice was hair removed, illuminated with either sham light or NAFL, and then inserted with two 5× base OVA-MNs (10 μg of OVA in total) or one flu-MNs (0.4 μg of HA equivalent PR8 vaccine) per mouse. For ID injection, one vaccine-packaged array was dissolved in 20 μL of PBS before ID injection into the skin. The blood samples were collected 7 and 28 d after immunization for evaluating cellular and humoral immune responses, respectively. Five weeks after immunization, the immunized and control mice were challenged by intranasal instillation of 5,000× LD_{50} mouse-adapted A/Puerto Rico/8/1934 H1N1 virus. For heterologous challenges, mice were intranasally instilled with mouse-adapted A/California/7/2009 H1N1, A/New Caledonia/20/1999 H1N1 or A/Aichi/2/68 H3N2 virus at a dose of 10× LD_{50} per mouse, respectively. Body weight and survival were monitored daily for 14 d unless otherwise specified.

For swine immunization, the animals were anesthetized by IM injection of telazol (2.2 mg kg^{-1})/xylazine (2.2 mg kg^{-1})/atropine (0.04 mg kg^{-1}) and maintained under isoflurane (2–3%) inhalation

during hair removal and immunization. Immunization procedure was similar as described in mice with two arrays each containing 1 μg HA content influenza vaccines inserted or inoculated into the exterior hind leg skin either alone or in the presence of NAFL. Seasonal influenza vaccine (2013–2014) at 2 μg of HA per animal was used for assessing skin reactogenicity. To quantify skin reactogenicity, the inoculation sites were photographed at indicated times.

Hemagglutination Inhibition (HAI) Assays. HAI titers were assayed according to a published protocol (10). Briefly, serum samples were incubated with receptor-destroying enzyme (RDE) (Denka Seiken) at 37 °C overnight followed by heat inactivation at 56 °C for 30 min. The resultant serum samples were incubated with 4 hemagglutination (HA) units of influenza virus at 37 °C for 1 h after serial dilutions of the serum sample, and then with 0.5% chicken red blood cells (Charles River Laboratories) at room temperature for 30 min. The HAI titer was defined as the reciprocal of the highest serum dilution that inhibited 4 HA units.

The ELISA. HA-specific IgG, IgG1, IgG2a, and IgA antibody titers were measured by ELISA. In brief, 1 μg/mL recombinant HA was coated overnight onto ELISA plates in $NaHCO_3$ buffer, pH9.6. The plates were incubated for 2 h with serially diluted serum samples, after which HRP-conjugated goat anti-mouse IgG (NA931V, GE healthcare, dilution 1:6,000), IgG1 (A90-105P, Bethyl, dilution 1:10,000), IgG2a (61-0220, Life Technologies, dilution 1:2,000) or IgA (A90-103P, Bethyl, 1:10,000) antibody was added to measure specific subtypes. For C57BL/6 mice, anti-mouse IgG2c (1079-05, Southern Biotech, 1:5,000) antibody was used in place of anti-IgG2a antibody.

Cell-Mediated Immune Responses. Peripheral blood mononuclear cells (PBMCs) were isolated from blood after red blood cell lysis. PBMCs at 10^6 cells mL^{-1} were incubated with influenza vaccine (1 μg mL^{-1} HA content) and anti-CD28 (clone 37.51, BD Pharmingen) antibody (4 μg mL^{-1}) overnight. Golgi-Plug (BD Pharmingen) was added to the culture in the final 5 h of the incubation. The stimulated cells were stained with fluorescence-conjugated antibodies against CD4 (clone RM4-5, Biolegend, dilution 1:100), CD8 (clone 53–6.7, Biolegend, dilution 1:200), and IFNγ (clone XMG1.2, Biolegend, 1:100) and subjected to flow cytometric analysis.

Quantitative Real-Time PCR. The skin were treated with NAFL or sham light, and injected with Hanks' Balanced Salt solution (HBSS), chloroquine (200 mM in HBSS, 50 μL) or DNase I (2,500 U in HBSS). The full thickness about 7×10 mm^2 of the NAFL-treated area was excised, and total RNA was extracted, reverse-transcribed, and amplified by real-time qPCR using a SYBR Green PCR kit (Roche). Glyceraldehyde 3-phosphate dehydrogenase (GAPDH) was used as an internal control. The primers were forward, atcaagaaggtggtgaagca, and reverse, agacaacctggtcctcagtgt for Gapdh; and forward, agctccaagaaaggacgaaca, and reverse, gccctgtaggtgaggttgat for Ifnb1.

Statistical Analysis. Data are presented as mean ± SEM. Two-tailed *t* test (*t* test) was used to analyze a difference between two groups, and one-way ANOVA was used among multiple groups. Log-rank test was used to analyze the survival. *P* value was calculated by PRISM software (GraphPad) and a difference was regarded significant if *P* value was less than 0.05.

1. Sato M, et al. (2000) Distinct and essential roles of transcription factors IRF-3 and IRF-7 in response to viruses for IFN-alpha/beta gene induction. *Immunity* 13(4):539–548.
2. Honda K, et al. (2005) IRF-7 is the master regulator of type-I interferon-dependent immune responses. *Nature* 434(7034):772–777.
3. Ishikawa H, Ma Z, Barber GN (2009) STING regulates intracellular DNA-mediated, type I interferon-dependent innate immunity. *Nature* 461(7265):788–792.
4. Boes M, et al. (2002) T-cell engagement of dendritic cells rapidly rearranges MHC class II transport. *Nature* 418(6901):983–988.
5. Wang J, Shah D, Chen X, Anderson RR, Wu MX (2014) A micro-sterile inflammation array as an adjuvant for influenza vaccines. *Nat Commun* 5:4447.
6. Yang SY, et al. (2013) A bio-inspired swellable microneedle adhesive for mechanical interlocking with tissue. *Nat Commun* 4:1702.
7. Sullivan SP, et al. (2010) Dissolving polymer microneedle patches for influenza vaccination. *Nat Med* 16(8):915–920.
8. Chen X, Kositratna G, Zhou C, Manstein D, Wu MX (2014) Micro-fractional epidermal powder delivery for improved skin vaccination. *J Control Release* 192:310–316.
9. Chen X, et al. (2010) A novel laser vaccine adjuvant increases the motility of antigen presenting cells. *PLoS ONE* 5(10):e13776.
10. Cottey R, Rowe CA, Bender BS (2001) Influenza virus. *Curr Protoc Immunol* 19:Unit 19.11.

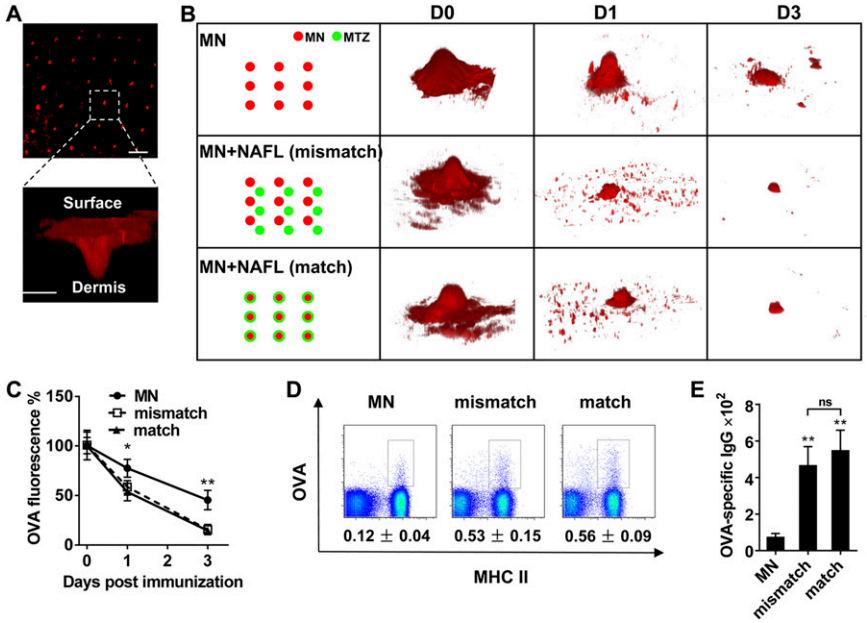

Fig. S1. NAFL enhances antigen delivery and humoral immune response independently of how MNs and MTZs are paired. (*A*) Delivery of OVA-AF647 (red) into the skin by MNs. One representative 3D fluorescent image of OVA delivered by a single microneedle is shown. (Scale bar, 1 mm in *Upper* and 200 μm in *Lower*.) (*B*) Real-time monitor of OVA distribution in the skin by 3D scanning. The mice were immunized by a 6 × 9 OVA-MNs alone (MN) or the MNs into NAFL-treated skin with MNs (red dots) mismatching (mismatched) or precisely matching (matched) MTZs (green dots) as illustrated in first column. OVA distribution in the skin was 3D scanned from day0 (D0) to day3 (D3). The 3D scanning was also used to measure the amount of OVA in the skin, which was summarized in *C*. $n = 10$. (*D*) Quantification of OVA+APCs in draining lymph nodes by flow cytometry. $n = 6$. (*E*) Serum OVA specific antibody is increased by NAFL. OVA-specific antibody was measured in serum by ELISA two weeks after immunization. $n = 6$. $^*P < 0.05$, $^{**}P < 0.01$, $^{***}P < 0.001$. All experiments were repeated twice with similar results.